

Deep Learning Framework for Accurate Prediction and High-Throughput Search of the Thermoelectric Figure of Merit in Skutterudites

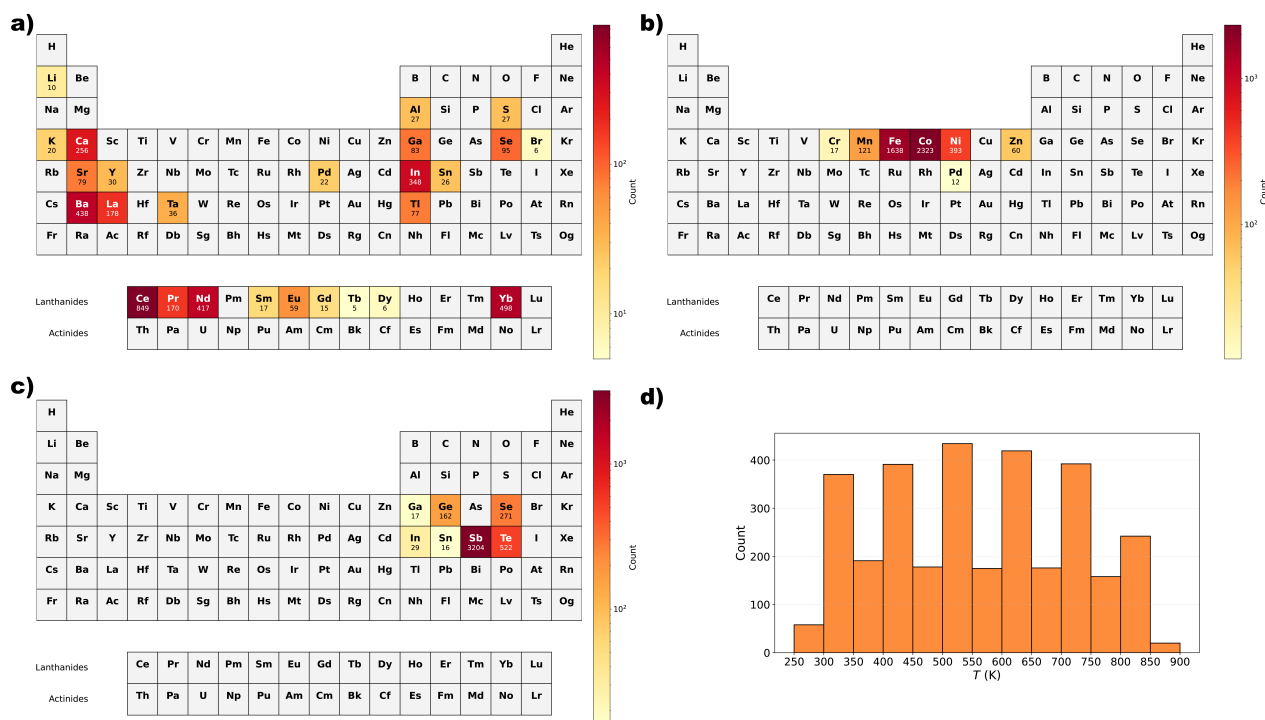


Figure S1. Compositional variability for training set of a) fillers, b) cations and c) anions. d) Temperature histogram of the training dataset.

Table S1. List of all descriptors used in the model, including structural, electronic, thermal and compositional features.

Structural Composition	
Descriptor	Meaning
num_anions	Number of anion species
num_cations	Number of cation species
num_fillers	Number of filler species
Electronegativity	
aver_a_elecneg	Average electronegativity of anions
dev_a_elecneg	Standard deviation of electronegativity among anions
aver_c_elecneg	Average electronegativity of cations
dev_c_elecneg	Standard deviation of electronegativity among cations
aver_f_elecneg	Average electronegativity of fillers
dev_f_elecneg	Standard deviation of electronegativity among fillers
Ionization Potential	
aver_a_ip	Average ionization potential of anions
dev_a_ip	Standard deviation of ionization potential among anions
aver_c_ip	Average ionization potential of cations
dev_c_ip	Standard deviation of ionization potential among cations

aver_f_ip	Average ionization potential of fillers
dev_f_ip	Standard deviation of ionization potential among fillers
Electron Affinity	
aver_a_ea	Average electron affinity of anions
dev_a_ea	Standard deviation of electron affinity among anions
aver_c_ea	Average electron affinity of cations
dev_c_ea	Standard deviation of electron affinity among cations
aver_f_ea	Average electron affinity of fillers
dev_f_ea	Standard deviation of electron affinity among fillers
Mass and Stoichiometry	
f_mass	Total mass of filler atoms in the structure
total_mass	Total atomic mass of all atoms in the system
std_dev_f_mass	Standard deviation of atomic mass among filler species
std_dev_a_mass	Standard deviation of atomic mass among anion species
std_dev_c_mass	Standard deviation of atomic mass among cation species
std_dev_f_frac	Standard deviation of atomic fraction among fillers
std_dev_a_frac	Standard deviation of atomic fraction among anions
std_dev_c_frac	Standard deviation of atomic fraction among cations
sum_f_frac	Sum of atomic fractions of all filler species
sum_a_frac	Sum of atomic fractions of all anion species
sum_c_frac	Sum of atomic fractions of all cation species
ratio_a_c	Ratio of the total atomic fraction of anions to cations
Electronic and Thermal Properties	
total_val_e	Total number of valence electrons in the system
n_300	Carrier concentration at 300 K
T	Temperature (K)
p_n	Carrier type (0 for p-type, 1 for n-type)
ZT	Thermoelectric figure of merit

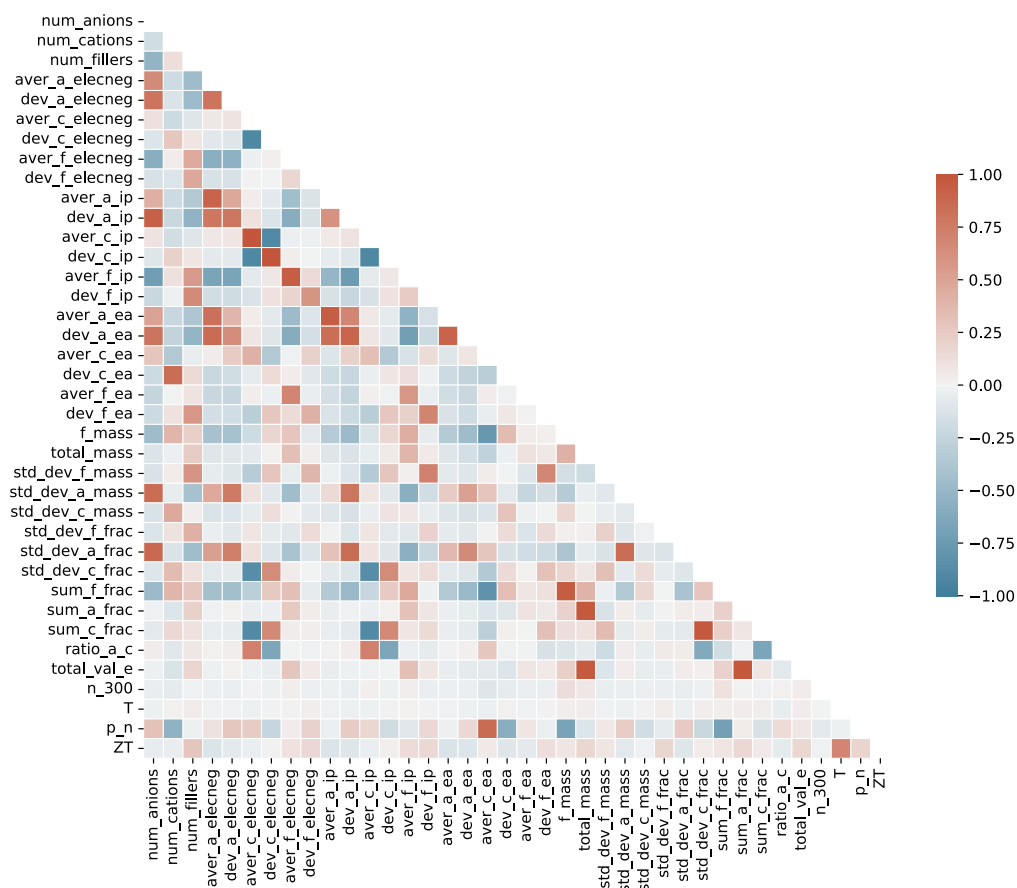


Figure S2. Pearson correlation matrix for all 37 descriptors and target zT used in model training.

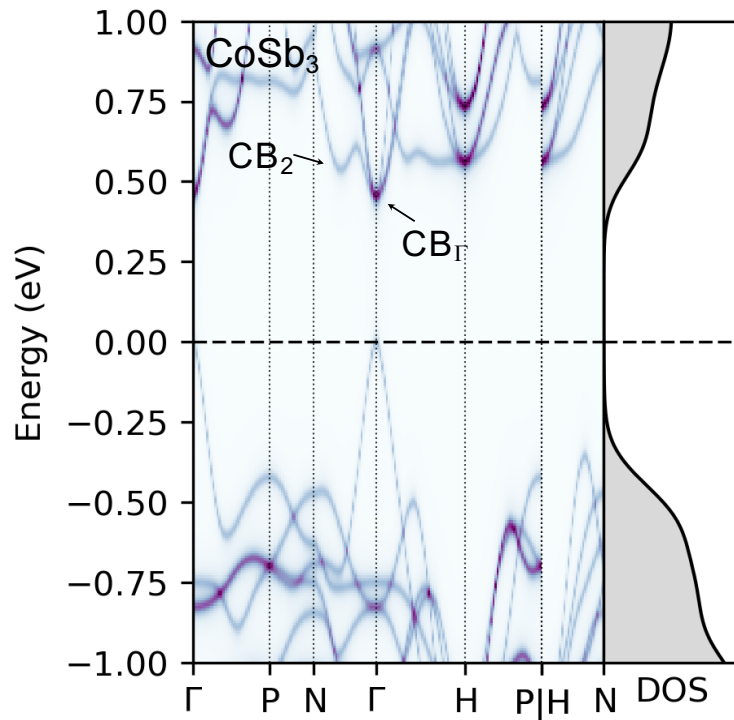


Figure S3. Unfolded band structure of pristine CoSb_3 used as reference for comparison with doped systems.

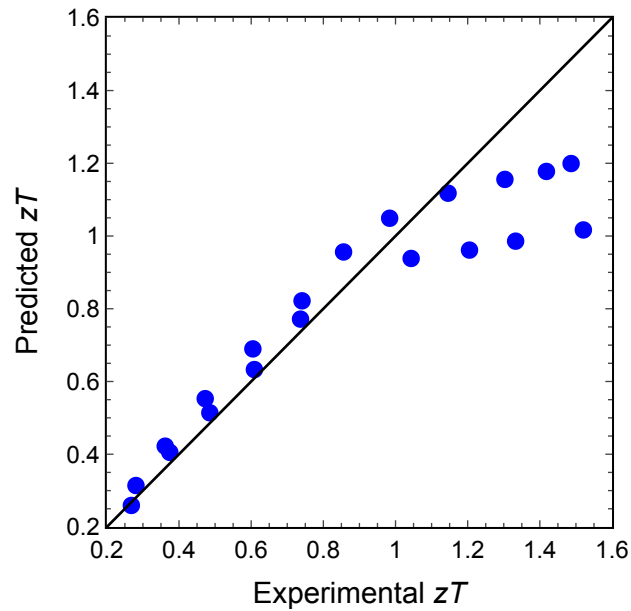


Figure S4. Predicted zT values for the $\text{S}_{0.2}\text{Se}_{0.05}\text{CoSb}_{11.25-2x}\text{Te}_{0.75}(\text{GeTe})_x$ samples synthesized by Wang et al [1].

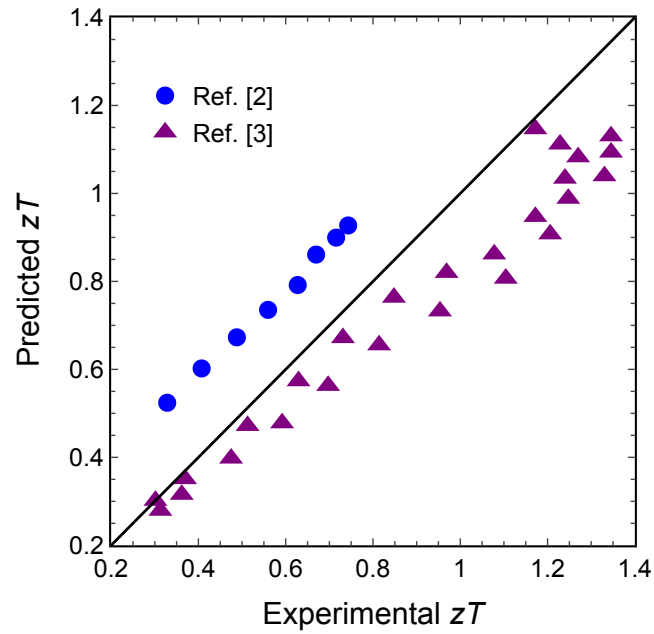


Figure S5. Predicted zT values for the composition $Yb_{0.12}Ca_{0.15}Co_4Sb_{12.09}$ (blue dots) reported by Salvador et al. [2] and for the $Y_xYb_{1-x}Co_4Sb_{12}$ (purple triangles) reported by Qin et al. [3].

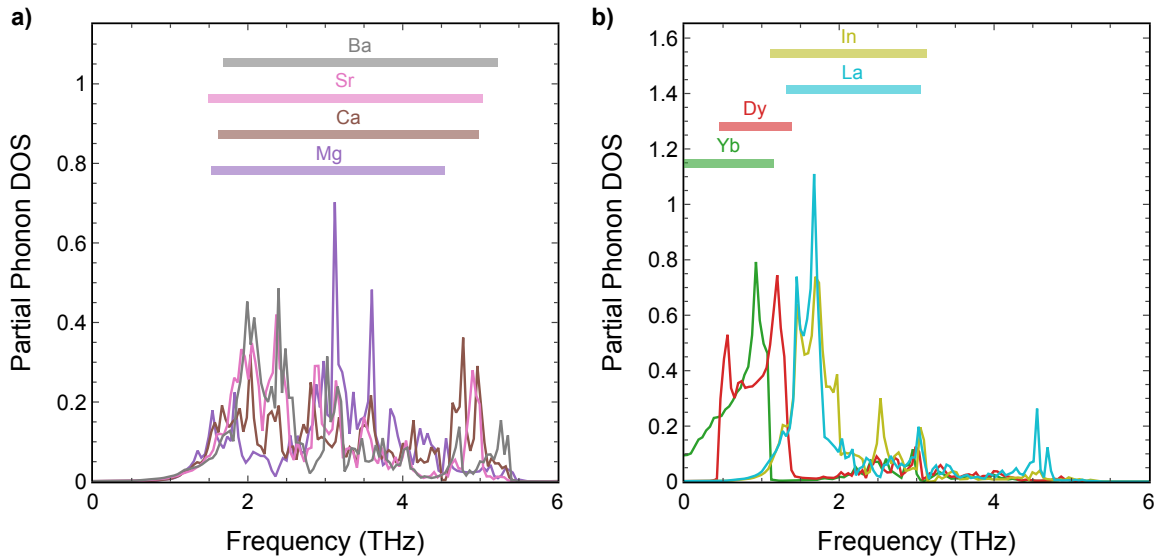


Figure S6. Projected phonon density of states for rattler atoms a) Mg (purple), Ca (brown), Sr (pink), Ba (grey), and b) Yb (green), Dy (red), In (yellow), La (light blue) in selected double-filled Co_4Sb_{12} -based skutterudites. The distinct peaks in the low-frequency region (<2 THz) in both a) and b) suggest localized vibrational modes. These results support the presence of dual-frequency resonant phonon scattering, as discussed in Figure 7 in the main text.

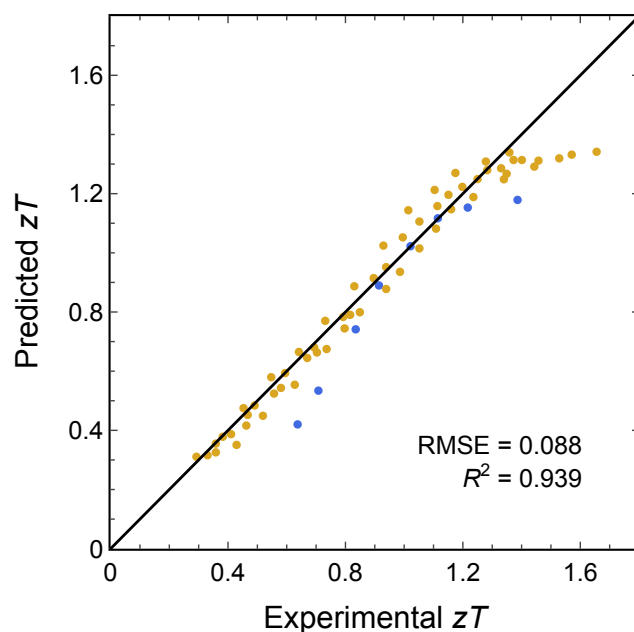


Figure S7. Predicted versus experimental zT values for high-performance *n*-type skutterudites containing multiple fillers. Systems from Ref. [4] (blue) and Ref. [5] (yellow) show agreement with model predictions. These compounds incorporate 3 or 4 different rattlers with distinct resonant frequencies, maximizing phonon scattering.

References

- [1] Y. Wang, J. Wang, X. Xu, Y. Wang, B. Jia, S. Li, K. Nielsch and J. He, *Adv. Energy Mater.*, 2026, 16, e05077.
- [2] J. Salvador, J. Yang, H. Wang and X. Shi, *J. Appl. Phys.*, 2010, 107, 043705.
- [3] D. Qin, W. Shi, X. Wang, C. Zou, C. Shang, X. Cui, H. Kang, Y. Lu and J. Sui, *Inorg. Chem. Front.*, 2024, 11, 1724–1732.
- [4] G. Rogl, A. Grytsiv, K. Yubuta, S. Puchegger, E. Bauer, C. Raju, R. Mallik and P. Rogl, *Amer. Mineral.*, 2015, 95, 201–211
- [5] X. Shi, J. Yang, J. R. Salvador, M. Chi, J. Y. Cho, H. Wang, S. Bai, J. Yang, W. Zhang and L. Chen, *J. Am. Chem. Soc.*, 2011, 133, 7837–7846.